Chapter 6

EEG and EMG Scalogram-based Hand Movement Classification using Transfer Learning

Abstract

This chapter presents the classification of hand movements using transfer learning by combining electromyography (EMG) and electroencephalography (EEG) scalograms. Initially, machine learning classifiers achieved a 74.96% accuracy in categorizing combined EEG and EMG signals. The study then investigated the impact of four scalogram types—Shannon, frequency B-spline, Mexican hat, and complex Gaussian—revealing that employing scalograms in conjunction with a convolutional network algorithm significantly improved accuracy to 91.31%. Through the integration of transfer learning, the classification accuracy was further raised to 97.57% with the VGG19 model, particularly when utilizing the Shannon scalogram, which emerged as the most effective. This methodology highlights the potential of fusing EEG and EMG signals for precise classification, with significant implications for brain-computer interfaces (BCIs), neuroprosthetics, assistive technology, and motor rehabilitation. The utilization of transfer learning to accurately classify hand movements demonstrates its capacity to greatly enhance the functionality of neuroprosthetic devices, BCIs, and related assistive and rehabilitation technologies

6.1 Introduction

Electroencephalography (EEG) is a non-invasive technique that involves recording the electrical activity generated by neurons in the brain, offering insights into cognitive processes, motor intentions, and emotional states (Teplan, 2002). EEG captures brain signals that can be translated into commands for external devices or computer interfaces. BCI is a technology that establishes direct communication pathways between the human brain and external devices (Värbu et al., 2022). It allows individuals with motor impairments to control, communicate, or interact with technology directly through their brain signals (Abiri et al., 2019). It enables users to express their thoughts, emotions, and intentions in real-time, allowing improved communication and social interaction (Torres et al., 2020). EEG-based BCIs are portable, versatile, and essential components of research and applications to enhance the quality of life for individuals with disabilities (Guger et al., 1999). As research and innovation in BCIs continue to advance, the potential to improve the lives of those affected by motor disabilities becomes increasingly tangible. Electromyography (EMG) signals are becoming increasingly popular for controlling devices due to their ability to capture human motion intention and muscle activity accurately. Hence, they can be utilized to provide adaptable commands for precise device control (Ahsan et al., 2009; Kaur, 2021; Lucas et al., 2004). EMG-based control systems have been successfully implemented in applications like wheelchairs, prosthetics, and exoskeletons, with remarkable results highlighting their crucial role in improving the quality of life for individuals with physical limitations (Fleming et al., 2021; Fonseca et al., 2019; Crawford et al., 2005).

6.2 Transfer Learning

Transfer learning is a crucial aspect of deep learning. It enables models to draw insights from one domain and apply them to entirely different ones. This process consists of two

essential phases: pretraining and fine-tuning (Zhuang et al., 2020). The initial pretraining phase involves training the model on a vast and varied dataset to ensure robust performance. This enables the model to extract complex features, leading to a better understanding of the data and an improved ability to generalize new examples. An unsupervised learning process enables the model to acquire considerable domain-specific knowledge. This phase is crucial because the model can learn to generalize the target task well, even if there is a shortage of labeled data. The pre-trained model moves into the fine-tuning phase, further refining its parameters. In this phase, the model is trained on a specific dataset, enabling it to adapt to the unique qualities of the target data while retaining its existing knowledge. The fine-tuning process is supervised learning, where the model is trained on labeled data to optimize its performance on the target task (Yang, 2020). An alternative fine-tuning approach is using the pre-trained model as a fixed feature extractor. This approach involves directing the intermediate representations from specific layers of the pre-trained model to an independent classifier or regression model (Neyshabur et al., 2020). The intermediate representations capture the high-level features of the input data, which can be used as input to other models. This framework uses robust and powerful architectures to facilitate knowledge transfer, including VGG16, VGG19, ResNet50, Inceptionv3, InceptionResNet, MobileNet, MobileNetv2, and DenseNet (Chen et al., 2021). The VGG16 and VGG19 models are renowned for their simplicity and consistency. They feature a series of convolutional layers followed by fully connected layers, all while maintaining a uniform input size (Simonyan and Zisserman, 2014). The ResNet50 model pioneered the concept of residual learning, utilizing skip connections to enable the training of deep networks (Mukti and Biswas, 2019). In contrast, the Inceptionv3 and InceptionResNet models introduced the inception module, which cleverly accommodates various filter sizes in parallel to capture information at multiple scales (Dong et al., 2020). The MobileNet and MobileNetv2 models were explicitly designed for mobile and embedded devices, achieving high performance through

depth-wise separable convolutions (Howard et al., 2017). In addition, incorporating DenseNet's dense connectivity patterns enhances feature reuse and reduces parameter overhead (Zhu and Newsam, 2017). These architectural choices have repeatedly proven effective and adaptable across various computer vision tasks, including image classification and feature extraction (Shin et al., 2016; Farahani et al., 2020). Thus, Cross-domain knowledge incorporation enhances classification tasks, enabling efficient training between related domains (Salehi et al., 2023).

6.3 Research Gap

The limitations of EEG for brain-computer interfaces include limited spatial resolution, susceptibility to interference, and the need for sophisticated processing techniques and customized setups. Furthermore, the relatively low signal-to-noise ratio poses challenges in achieving accuracy and reliability, emphasizing the need for innovative approaches to harness BCI technology fully. EMG is crucial for assessing muscle function and diagnosing neurological disorders. However, it faces challenges in capturing subtle movements and may produce weak signals in individuals with certain neuromuscular disorders, affecting its reliability over time. EEG and EMG are susceptible to cross-talk, which refers to the unwanted interference of electrical signals from neighboring sources. In EEG, cross-talk often results from adjacent electrodes picking up electrical activity from unintended sources such as muscle contractions, eye blinks, and movements. In EMG, cross-talk occurs when signals from one muscle recording site are contaminated by electrical activity from neighboring muscles. Careful electrode placement and advanced signal processing techniques like filtering and source localization are necessary to reduce cross-talk. Failing to address cross-talk can lead to misinterpretation of data, potentially impacting patient treatment and rehabilitation outcomes. In EEG and EMG research, inter-subject variability is a crucial factor. It reflects inherent differences in electrical activity among individuals,

arising from brain structure, age, genetics, and cognitive state in EEG, as well as muscle structure, size, body composition, and motor control in EMG.

6.4 Proposed Solution

Neuromuscular activity classification in BCI and neuroprostheses is challenging due to the limitations of EEG and EMG signals (Elsayed et al., 2017; Enders & Nigg, 2016). However, scalograms can effectively overcome these limitations and improve classification accuracy. Scalograms transform the signals in the time-frequency domain and help identify hidden signal patterns; additionally, they can reduce the impact of noise (Narin, 2022; Alyasseri et al., 2019). In the present study, deep convolutional networks and transfer learning are utilized to accurately classify EEG-EMG scalograms and distinguish between two hand movements (hand close and hand open). The study evaluated hand movement classification using EEG and EMG data, applying machine learning algorithms, deep convolutional networks and transfer learning. The performance of different classifiers and established networks was evaluated for general hand movements, left and right hand classification.

6.5 Materials and Method

6.5.1 Data Collection

Fifteen healthy participants, four females and eight males without neurological or physical conditions, were enrolled in this study. The average age of the participants was (25 ± 5) years, with an average weight of (70 ± 15) kg and an average height of (160 ± 12) cm. EEG data was gathered utilizing a 32-channel ActiCap with a BrainVision LiveAmp amplifier, according to the standard 10-20 montage scheme. Data from nine

channels over the sensorimotor cortex were recorded at a sampling frequency of 1000 Hz. Electrode impedance was consistently maintained below 25 kΩ to preserve data quality. The BrainVision recording software applied a software-based bandpass filter with a 4–30 Hz frequency range to eliminate artifacts related to eye blinks, facial muscle movement, and power line noise. This filtering process preserved only the delta, alpha (also known as mu in the context of motor-related events), and beta frequency bands pertinent to motor processes. The original sampling frequency for EMG data was 1926 Hz, resampled to 1000 Hz for compatibility with EEG data. A bandpass filter ranging from 20 to 450 Hz was used for EMG signal acquisition using the Delsys Trigno wireless system. Figure 6.1(a) illustrates the data collection setup, while Figure 6.1(b) presents the electrode position used in the study.

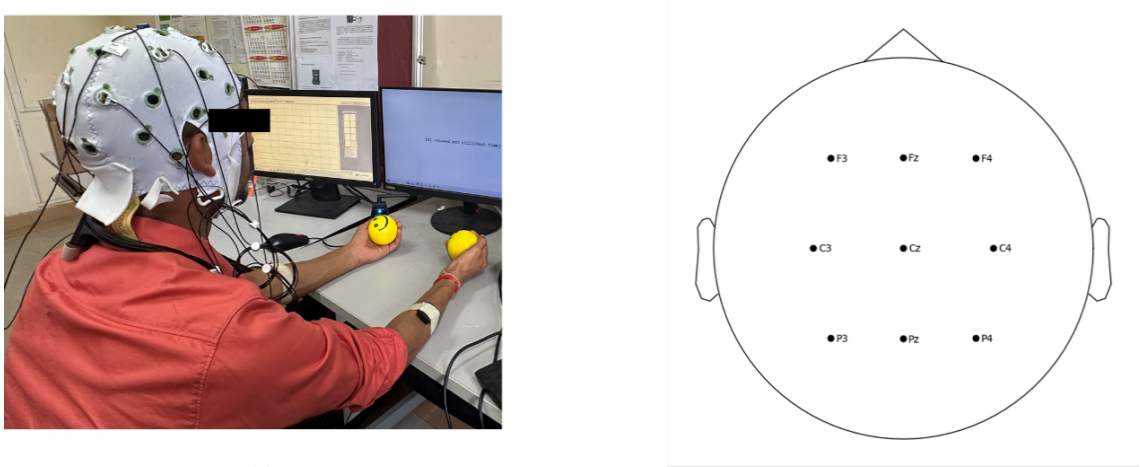

Fig. 6.1 (a) Experimental Setup. (b) EEG Electrode positions

Participants were seated approximately one meter from a screen, with their arms resting on their thighs or a table to minimize unnecessary arm movements. Task instructions were displayed on the screen after prior briefings and task rehearsals. Each participant completed four sessions lasting 6-8 minutes, with breaks in between. Each session had 30-second rest intervals within 3 trials involving hand movements. Each trial started with an 8-second preparation period, including a 3-second interval for eye blinking to prevent

artifacts. Participants focused on a central cross to maintain a steady gaze. Instructions to close and open the left or right hand for 3 seconds were presented randomly to avoid anticipation. The complete flow chart of the study is shown in Figure 6.2.

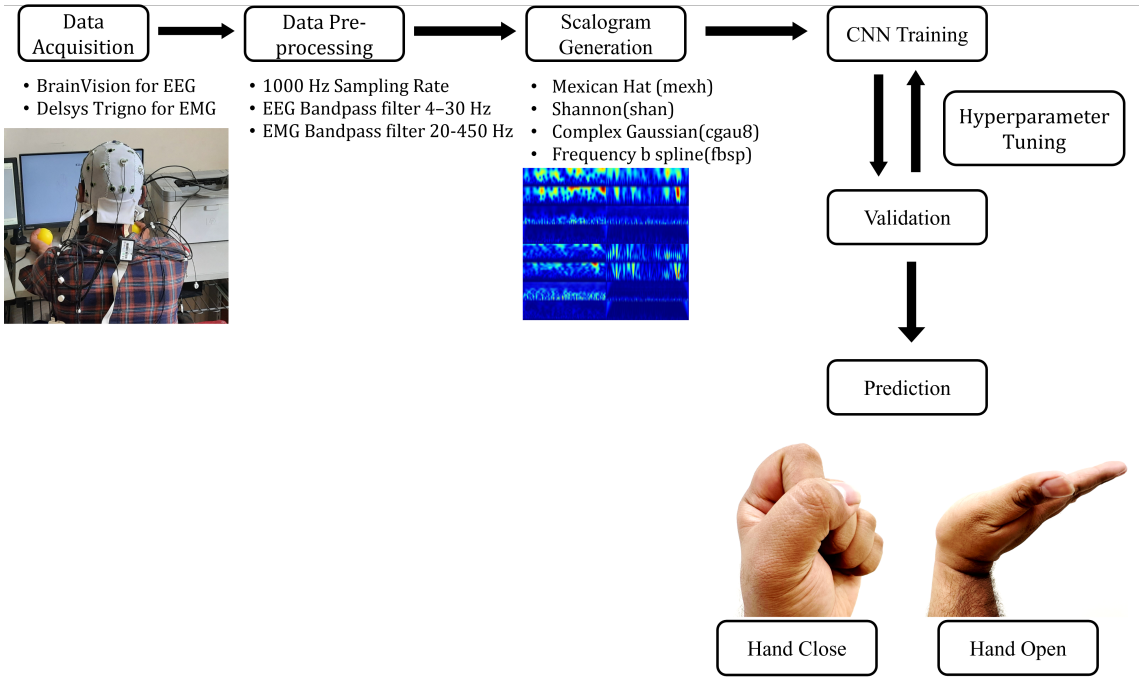

Fig. 6.2 Complete flowchart of the study

6.5.2 EEG Features

EEG signal analysis involves deriving a range of features that provide valuable insights into brain activity. These features include Mean Frequency (MNF), Median Frequency (MDF), Total Power (TTP), Mean Power (MNP), Spectral Moments 1, 2, and 3 (SM1, SM2, and SM3 respectively), as well as Variance Central Frequency (VCF). Mean frequency is the average frequency of the EEG signal, while Median Frequency is the midpoint frequency value. Total power quantifies the overall power distribution across all frequencies, while Mean Power calculates the signal's average power. Spectral Moments 1, 2, and 3 capture different aspects of the signal's spectral distribution, reflecting the moments about the mean frequency. Variance Central Frequency measures the variability in the central frequency.

Together, these features offer a comprehensive view of the frequency content and power distribution within EEG signals, enabling scientists to understand and analyze neural activity better. Power spectrum density was also analyzed for opening and closing the hand. Table 6.1 lists the formulae of the features used in the present study. f_i Is the frequency of the spectrum at frequency window i, P_i is the power spectrum at window i, M is the length of the window, and f_c is the central frequency of the signal.

Table 6.1 EEG features used in the present study

Name	***Equation***	***Description***
MNF	$\frac{\sum_{i=1}^{M} f_i P_i}{\sum_{i=1}^{M} P_i}$	The average EEG signal frequency indicates the central tendency of the signal's frequency content.
MDF	$\frac{1}{2}\sum_{i=1}^{M} P_i$	It represents the frequency at which half of the signal's power is below, and half is above.
TTP	$\sum_{i=1}^{M} P_i$	The overall power distribution across all frequency components in the EEG signal. It quantifies the total energy or strength of the signal.
MNP	$\frac{\sum_{i=1}^{M} P_i}{M}$	The average power of the EEG signal provides a measure of the signal's overall power content.
SM1	$\sum_{i=1}^{M} f_i P_i$	A measure of the signal's first spectral moment indicates the spectral power's concentration or spread.
SM2	$\sum_{i=1}^{M} f_i P_i^2$	A measure of the signal's second spectral moment, signifying the spectral bandwidth or width of the EEG signal.
SM3	$\sum_{i=1}^{M} f_i P_i^3$	A measure of the signal's third spectral moment, reflecting skewness or asymmetry in the signal's spectral distribution.

6.5.3 EMG Features

The EMG features used in the present study are Root Mean Square (RMS), Mean Absolute Value (MAV), Variance (VAR), Skewness, Kurtosis, and Coefficient of Variation (CV). Table 4 lists the details of the features used in the present study. In Table 6.2, x represents

the input sample, N represents the total number of samples, and μ represents the mean. Further, the signal underwent the Continuous Wavelet Transform (CWT), a mathematical method that transforms signals into the time-frequency domain by convolving them with a set of wavelet functions that are scaled and shifted. This is used to generate a scalogram, a two-dimensional plot that illustrates the magnitude of wavelet coefficients with time on the x-axis and frequency on the y-axis. The scalogram provides a comprehensive view of signal features, making it a valuable tool for signal analysis. For this study four wavelet functions (Complex Gaussian, Frequency B Spline, Mexican Hat, and Shannon) as well as their combination was used.

Table 6.2 EMG features used in the present study

Name	***Equation***	***Description***
MAV	$\frac{1}{N}\sum_{i=1}^{N}\lvert x_i\rvert$	The MAV can assess muscle activation during different tasks or movements.
RMS	$\sqrt{\frac{1}{N}\sum_{i=1}^{N}x_i^2}$	The RMS assesses muscle fatigue or changes in muscle activity over time.
VAR	$\sqrt{\frac{\sum_{i=1}^{N}(x_i-\mu)}{N}}$	The variance can be used to assess the stability of muscle activity during movements.
Skewness	$\frac{1}{N}\sum_{i=1}^{N}\left(\frac{x_i-\mu}{\mathrm{Var}}\right)^3$	Skewness assesses changes in muscle activity during different phases of a movement or task.
Kurtosis	$\frac{1}{N}\sum_{i=1}^{N}\left(\frac{x_i-\mu}{\mathrm{Var}}\right)^4$	Kurtosis measures the muscle recruitment or coordination changes in the EMG signal distribution.
CV	$\frac{\mu}{\sigma}$	Relative variability in muscle activity amplitudes.

6.5.4 Machine Learning

The study involved classifying extracted features using various conventional machine-learning algorithms. K-Nearest Neighbors (KNN), Naïve Bayes (NB), Support Vector Machine (SVM) with three kernel functions (i.e., polynomial, linear, and radial basis function), Decision Tree (DT), Logistic Regression (LR), and Random Forest (RF) were

selected for classification. Machine learning algorithms are inherently parameterized, and the choice of hyperparameters significantly influences their performance. For example, in KNN, parameters such as the number of neighbors, weighting strategy, and algorithm type directly impact classification accuracy. SVM's regularization strength, denoted by 'C,' is adjustable, along with kernel-related parameters like gamma and degree. Decision Trees' parameters include maximum tree depth, minimum samples required for node splitting, and the minimum number of samples in a leaf node, all of which govern model complexity. Logistic Regression's regularization strength is determined by 'C,' and the penalty choice ('l1' or 'l2') dictates the type of regularization applied, while the solver specifies the optimization algorithm. Random Forest parameters encompass the number of trees in the forest, maximum tree depth, minimum samples for node splitting, and the minimum number of samples in a leaf node. An exhaustive grid search, coupled with a 5-fold cross-validation methodology, was executed to ensure a thorough exploration of each algorithm's performance. This approach was designed to assess algorithmic performance thoroughly across various scenarios and parameter settings.

6.5.5 Transfer Learning

Eight standard models were used for the transfer learning task. These are: VGG16, VGG19, ResNet50, Inceptionv3, InceptionResNet, MobileNet, MobileNetv2, and DenseNet Large. VGG16 and VGG19 are notable for their straightforward and uniform architecture consisting of multiple convolutional layers followed by fully connected layers. These models excel in extracting hierarchical features from images, making them effective choices for tasks requiring detailed feature representation. Figure 6.3 shows the working principle of transfer learning.

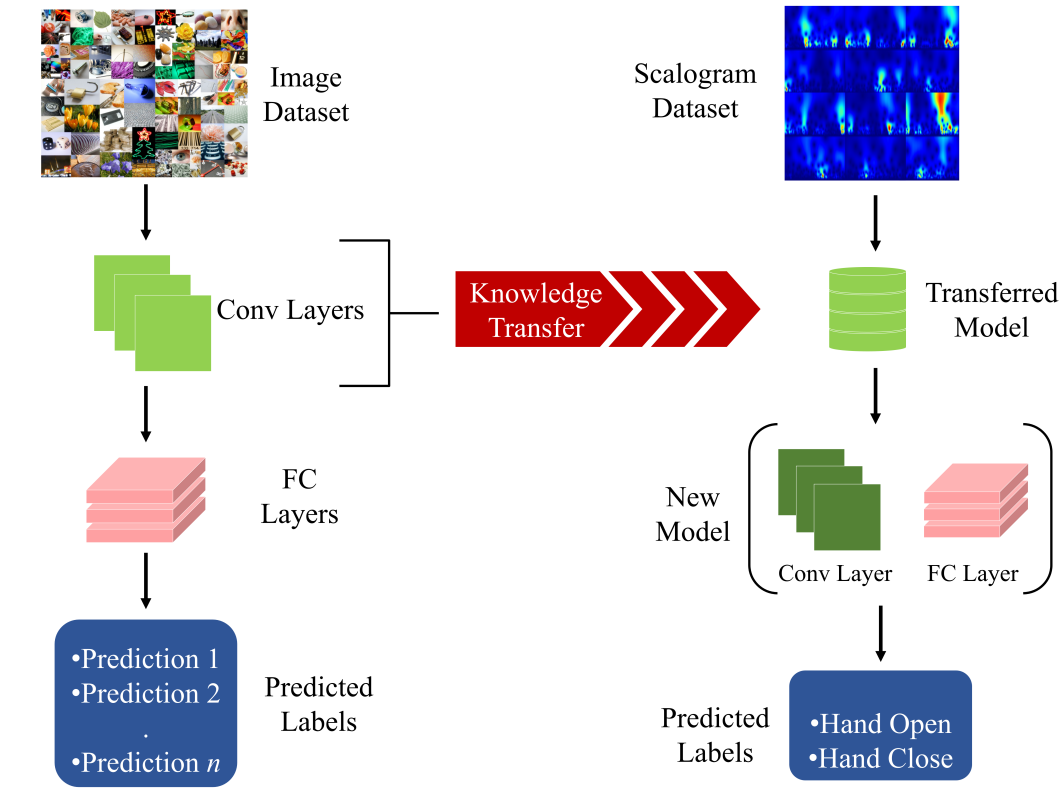

Fig. 6.3 Working principle of transfer learning

6.6 Results and Discussion

In Figure , the signal waveforms for EEG recorded at channels C3 and C4 and EMG signals are depicted for the opening and closing of the hand. Figure 6.4(a) shows the closing of the left hand, Figure 6.4(b) the opening of the left hand, Figure 6.4(c) the opening of the right hand, and Figure 6.4(d) the closing of the right hand. This allows direct observation of the electrical activity associated with the motor control and execution of these actions.

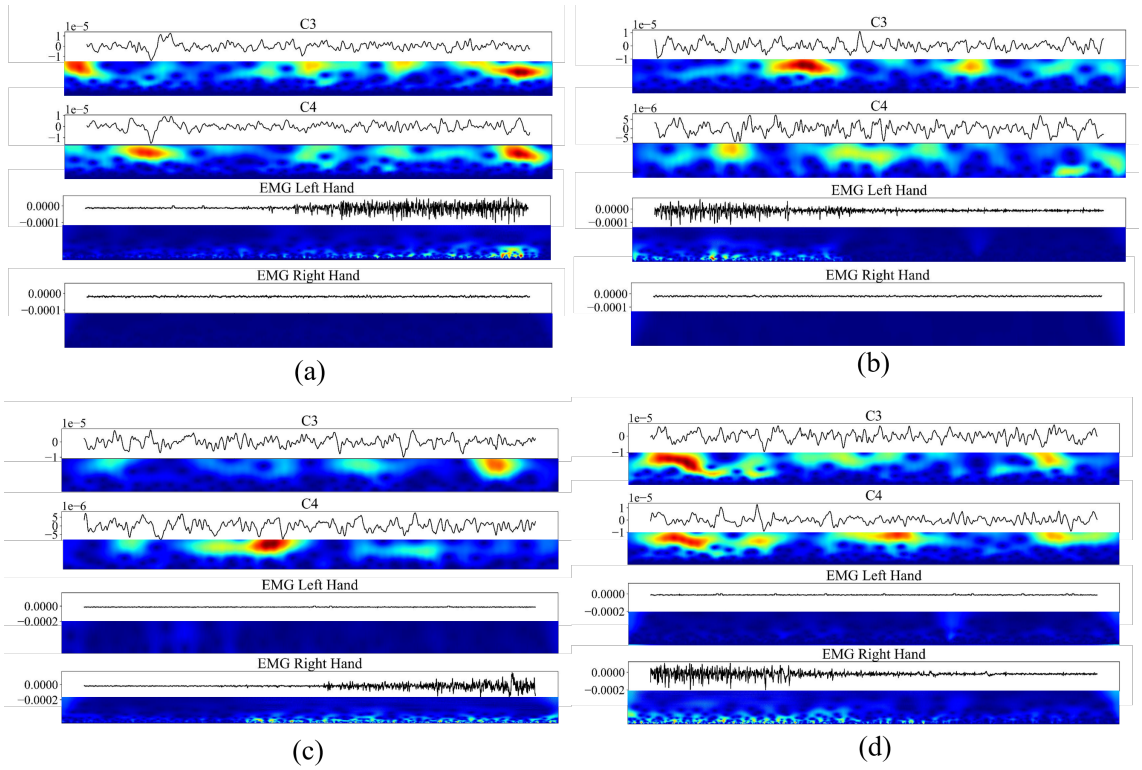

Fig. 6.4 Signal waveforms for C3 and C4 EEG and left and right-hand EMG for each movement. (a) Left hand closed, (b) Left hand open, (c) Right hand open, and (d) Right hand closed

The power spectral diagram for averaged trials presented in Figure 6.5 shows an apparent reduction in power at around 10 Hz during Hand Close trials, particularly in the C4 channel, compared to other hand movements. This reduction in power at this specific frequency suggests a unique neural and muscle activity pattern during Hand Close trials. The analysis of the features reveals distinct patterns in the frequency and power characteristics of open and closed hand trials within the C3 and C4 channels. The mean frequency in open-hand trials was significantly higher (12.18 Hz) than in closed-hand trials (11.13 Hz). The Median Frequencies also showed a similar trend, with 10.66 Hz and 9.66 Hz values for open and closed trials, respectively. These findings were supported by the lower power in the α band in hand close trails, as evidenced by the PSD plots. Additionally, the Mean Power (MNP) of hand open trials exceeded that of hand close trials in both C3

and C4, indicating a higher level of Event-Related Desynchronization (ERD) in hand close trials, as corroborated by the PSD plots. The feature boxplots are shown in Figure 6.6.

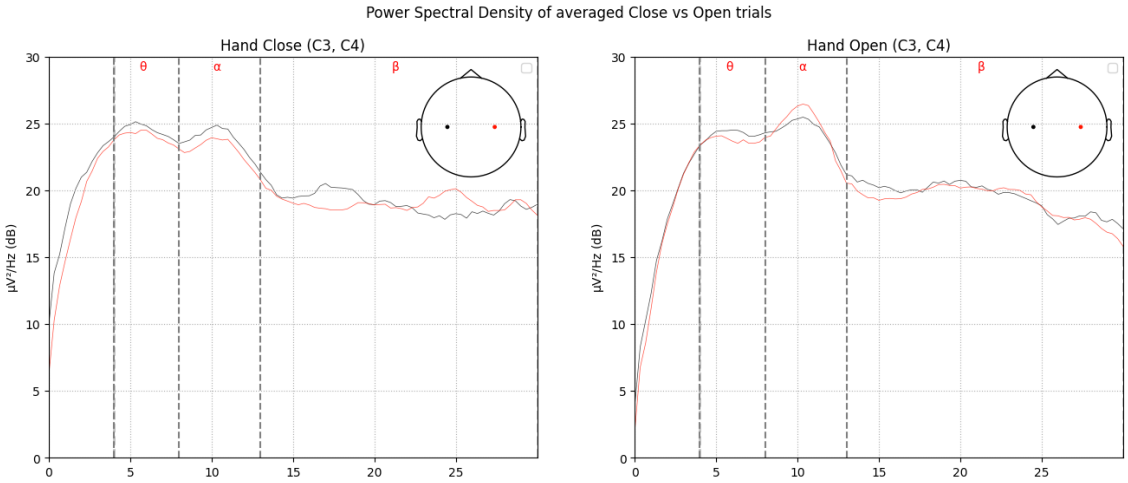

Fig. 6.5 PSD for hand close and open

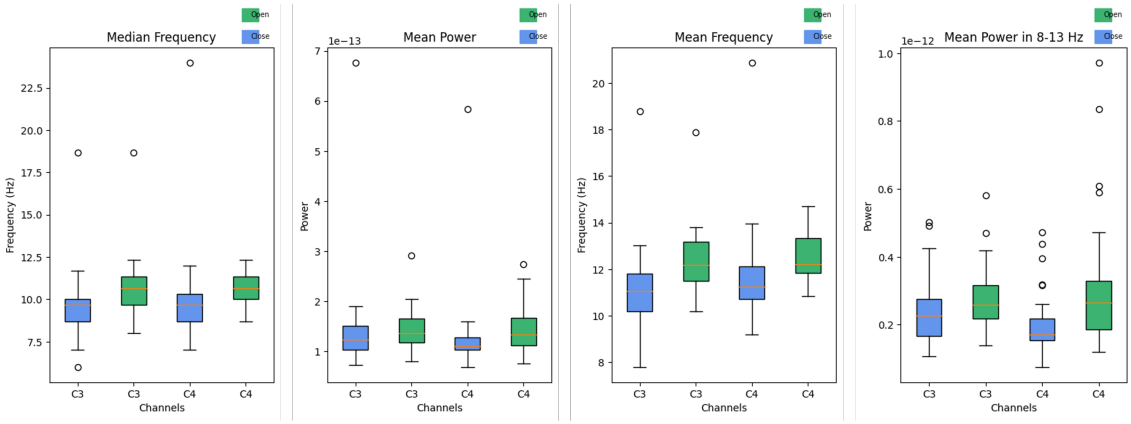

(a) (b) (c) (d)

Fig. 6.6 EEG features (a) Median Frequency, (b) Mean Power of the entire spectrum, (c) Mean Frequency, and (d) Mean Power of the α band (8-13 Hz)

The classification outcomes vary greatly depending on the modality and classification techniques used. When analyzing EEG signals alone, the accuracy achieved using a Support Vector Machine (SVM) Poly classifier with a window size 3000x1000 is only 33.99%. However, using the Random Forest Classifier (RFC) classifier with reduced window sizes of 2000x1000, the accuracy rates for left and right-hand gestures improved significantly to

75.13% and 77.42%, respectively. A summary of the EEG signal classification results is given in Table 6.3.

Table 6.3 Classification results for EEG signal using ML

Task	*Window*	*Classifier*	*Accuracy*	*Precision*	*Recall*	*F1*
Both Hands	3000x1000	SVM	33.99%	34.60%	33.76%	0.32
Left	2000x1000	RFC	75.13%	75.17%	75.03%	0.75
Right	2000x1000	RFC	77.42%	77.42%	77.43%	0.77

In contrast, combining EEG signals and EMG data and utilizing a Random Forest Classifier (RFC) with a window size of 2000x500 leads to improved results. Classification accuracy consistently reaches 74.96% for both hands, 75.20% for the left hand, and 77.42% for the right hand. Table 6.4 summarizes these findings, highlighting the significant advantages of fusing EEG and EMG data for classification purposes.

Table 6.4 Classification results for EEG combined with EMG signal using ML

Task	*Window*	*Classifier*	*Accuracy*	*Precision*	*Recall*	*F1*
Both Hands	2000x500	RFC	74.96%	75.01%	74.96%	0.74
Left	2000x500	RFC	75.20%	75.24%	75.10%	0.75
Right	2000x500	RFC	77.42%	77.44%	77.45%	0.77

Further, utilizing CNN-based classification of scalograms results in a noteworthy enhancement in EEG-only classification, particularly for the hand task, with an accuracy increase of up to 54.67%. However, it should be noted that the precision and recall levels remain moderate, suggesting that the model may be overfitting. In contrast, left-hand classification achieved 67.54% accuracy, and right-hand classification achieved 71.30% accuracy with comparable precision and recall. Table 6.5 displays the outcomes of the CNN classification of EEG scalograms. CNN proves to be an exceptional tool for classifying EEG and EMG scalograms together, as it achieves remarkable accuracy levels.

Table 6.5 Classification results for EEG scalogram using CNN

Task	*Accuracy*	*Precision*	*Recall*	*AUC*	*PRC*
Both Hands	54.67%	38.46%	31.70%	0.54	0.35
Left	67.54%	65.67%	62.32%	0.68	0.70
Right	71.30%	68.60%	70.50%	0.72	0.69

The accuracy for both hand tasks has surged to an impressive 91.31%, accompanied by high precision, recall, AUC, and PRC values of 91.79%, 89.24%, 0.95, and 0.9684, respectively. The accuracy levels for classifying left- and right-hand gestures are also notably high and are further supported by precision, recall, AUC, and PRC values. For the left hand, an accuracy of 95.10% was obtained, and for the right hand, 92.36% was achieved. The results are presented in Table 6.6.

Table 6.6 Classification results for combined EEG and EMG scalogram using CNN

Task	*Accuracy*	*Precision*	*Recall*	*AUC*	*PRC*
Both Hands	91.31%	91.79%	89.24%	0.95	0.9684
Left	95.10%	95.10%	95.10%	0.97	0.9746
Right	92.36%	92.36%	92.36%	0.97	0.9665

Figure 6.7 displays the classification results for each wavelet type and their performance in classifying individual left and right-hand movements. The "shan" scalogram achieved the highest accuracy at 97.40%, demonstrating its exceptional potential in capturing the distinctive features of these movements. Additionally, the "fbsp" and "mexh" scalograms also achieved commendable accuracy of 96.79% and 95.14%, respectively, showcasing their robustness in movement classification. The combined scalogram approach maintained a high classification accuracy of 94.88%, confirming the benefits of leveraging multiple scalograms for improved performance. Further, the "cgau8" scalograms showed potential with an accuracy of 93.92%, indicating its reliability for the task. The model also achieved an accuracy of 94.41% in distinguishing between left and right-hand movements, demon-

strating its ability to classify fine-grained hand movements. The achieved AUC and PRC values further highlight the robustness of the classification models.

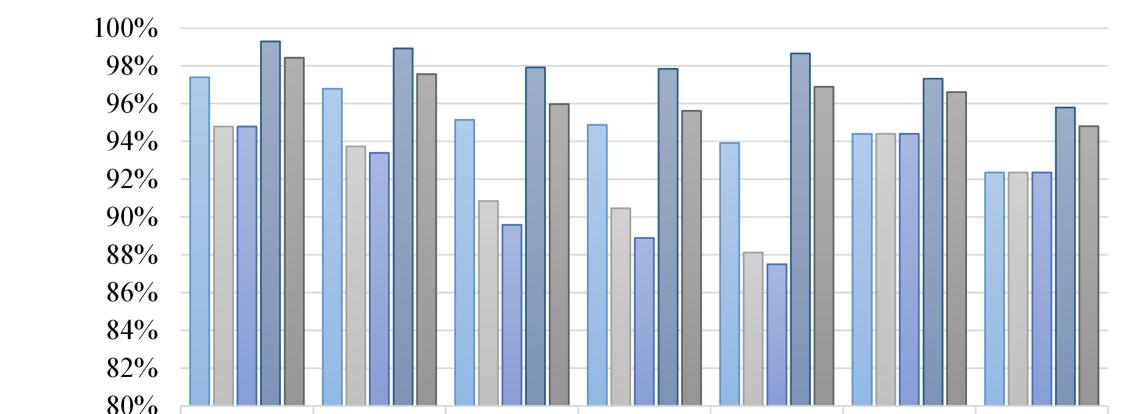

	shan	fbsp	mexh	Combined	cgau8	Left Hand	Right Hand
Accuracy	97.40%	96.79%	95.14%	94.88%	93.92%	94.41%	92.36%
Precision	94.79%	93.73%	90.85%	90.46%	88.11%	94.41%	92.36%
Recall	94.79%	93.40%	89.58%	88.89%	87.50%	94.41%	92.36%
AUC	0.9929	0.9893	0.9792	0.9784	0.9866	0.9733	0.958
PRC	0.9843	0.9756	0.9598	0.9562	0.9689	0.9662	0.9481

Fig. 6.7 Classification performance for different wavelets

Transfer learning models, including VGG19, ResNet50, DenseNet, MobileNet, VGG16, Inceptionv3, Inception-ResNet, and MobileNet v2, were employed for hand movement classification using EEG-EMG scalograms and CNNs. VGG19 achieved the highest accuracy of 97.57%, followed by ResNet50 with 97.40%. DenseNet and MobileNet also performed well, with accuracy above 96%. Inception-ResNet and MobileNet v2 had lower 92.27% and 86.11% accuracy respectively. The results demonstrate the efficacy of transfer learning in hand movement classification with potential applications in neuroprosthetics and brain-computer interfaces. Figure 6.8 summarizes the classification results for the transfer learning task.

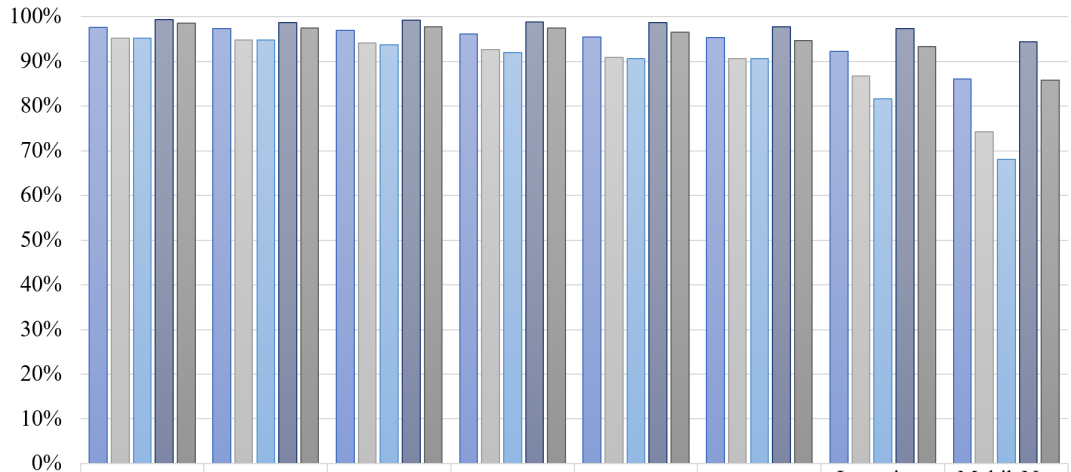

	VGG19	ResNet50	DenseNet	MobileNet	VGG16	Inceptionv3	Inception-ResNet	MobileNet v2
Accuracy	97.57%	97.40%	96.96%	96.18%	95.40%	95.31%	92.27%	86.11%
Precision	95.14%	94.79%	94.08%	92.66%	90.94%	90.62%	86.72%	74.24%
Recall	95.14%	94.79%	93.75%	92.01%	90.62%	90.62%	81.60%	68.06%
AUC	0.9941	0.9872	0.9917	0.9885	0.9871	0.9769	0.9733	0.944
PRC	0.9849	0.9752	0.9777	0.9742	0.9652	0.9464	0.9333	0.8576

Fig. 6.8 Classification results for Transfer Learning

6.7 Conclusion

This study addresses the challenges associated with EEG signal classification in Brain-Computer Interface (BCI) applications by utilizing Convolutional Neural Networks (CNNs) combined with scalograms and a fusion approach with EMG signals. The study showcases the potential for improving accuracy and reducing noise and variability in EEG signals. The integration of CNNs with scalograms resulted in more reliable classification. The combination of EEG and EMG signals, with or without CNN, consistently outperforms EEG-only approaches. This research also highlights the importance of the EEG-EMG fusion-based approach, which can be utilized in BCIs, neuroprosthetics, and motor imagery research. Further and transfer learning incorporation allow models to leverage knowledge from one problem to solve another related problem. Future research is aimed at expanding the datasets to evaluate model robustness. Overall, combining EEG and EMG scalograms

and classifying them through deep convolution networks and transfer learning holds significant promise for healthcare and assistive technology.